



Received on 29 November, 2017; received in revised form, 07 March, 2018; accepted, 11 March, 2018; published 01 July, 2018

## CARBON NANOTUBE USAGE IN MEDICAL APPLICATIONS - REVIEW

E. N. Ganesh

Vels Institute of Science, Technology and Advanced Studies, Pallavaram, Chennai - 600117, Tamil Nadu, India.

### Keywords:

Nanocomposites,  
Light Emitting Diode, Quasi  
ordering, Nanotube and Infrared

### Correspondence to Author:

**Dr. E. N. Ganesh**

Dean,  
Vels Institute of Science,  
Technology and Advanced Studies,  
Pallavaram, Chennai - 600117,  
Tamil Nadu, India.

**E-mail:** enganesh50@gmail.com

**ABSTRACT:** Bulk nanocomposites prepared from aqueous albumin dispersion with carbon nanotubes by removing the liquid component from the dispersion have been investigated. The composites were obtained by thermostating and exposure to LED and IR diode laser radiation. The nanocomposites obtained under laser irradiation retain their shape and properties for several years, in contrast to the composites fabricated in different ways (which decompose into small fragments immediately after preparation). The low density of the composites under study ( $\sim 1200 \text{ kg/m}^3$ ), which is close to the density of water, is due to their high porosity. The hardness of stable nanocomposites ( $\sim 300 \text{ MPa}$ ) was found to be at the same level as the hardness of polymethylmethacrylate, aluminium, and iron and close to the hardness of human bone tissue. The cluster quasi ordering of the inner structure of nanocomposites revealed by atomic force microscopy indicates the possibility of forming a bulk nanotube framework in them, which can be caused by the effect of the electric field of laser radiation and ensure their stability and hardness. The presence of a framework in nanocomposites provides conditions for self-assembly of biological tissues and makes it possible to apply laser-prepared nanocomposites as a component of surgical implants.

**INTRODUCTION:** Among the modern methods of bioengineering and medicine, which are aimed at protecting health and improving the quality of life of millions of people, increasing attention is paid to various ways of regenerating organs and tissues. A new interdisciplinary branch-tissue bioengineering-is an alternative to conventional transplantation of human organs. It aims at restoring the vital functions of the human organism through substitution of pathologically changed biological tissues, conservation of the substituent's, and provision of their functioning.

One of the main areas in tissue bioengineering is searching for methods for designing new imitative 3D structures - synthetic implants, which should stimulate growth and differentiation of cells during tissue formation <sup>1</sup>.

The characteristics of artificial implants (biocompatibility, biodegradability, porosity, size and connectivity of pores, immune response, *etc.*) must be no worse than those of the natural intercellular matrix. At the same time, wide application of high-strength metal (for example, titanium and its alloys) implants in tissue bioengineering is hindered by their low biodegradability and insufficiently high biocompatibility. Hydroxyapatite, calcium phosphate, and composites based on them, which have a developed porous structure and are good bone substituents are often used. However, these materials are low - tech and brittle <sup>2</sup>.

<b>QUICK RESPONSE CODE</b> 	<b>DOI:</b> 10.13040/IJPSR.0975-8232.9(7).2686-92
	Article can be accessed online on: <a href="http://www.ijpsr.com">www.ijpsr.com</a>
DOI link: <a href="http://dx.doi.org/10.13040/IJPSR.0975-8232.9(7).2686-92">http://dx.doi.org/10.13040/IJPSR.0975-8232.9(7).2686-92</a>	

Surgical application of carbon implants, which can withstand higher mechanical loads than bone transplants, accelerating synostosis and preventing resorption and bone fracture, was described in <sup>3</sup>. The use of highly porous cellular implants provides their direct, strong connection without a tissue interlayer. A drawback of carbon implants is their tendency to cause physical and biological changes in tissues <sup>4</sup>. To date, their application has been limited by inflammatory backbone diseases.

For the aforementioned reasons, interest has been shown in the fabrication and application of polymer based bulk structures; their advantage is the possibility of varying properties in wide limits by changing the material composition <sup>5</sup>. However, they have also a number of drawbacks. The widely used linear aliphatic polymers (polylactide, polyglycolic acid, and copolymers of milky and glycolic acids) have relatively low mechanical characteristics. Hydrogels (for example, polyethylene glycol) have strength similar to that of cartilaginous tissues; however, their biodegradability is rather low. On the whole, the properties of all these compounds are much inferior to the biological matrix parameters <sup>6</sup>.

All these factors are drawing researchers attention to the possibility of applying nanocomposites in surgical implantation; due to their novel properties, these materials are widely used in modern technologies, including biological applications <sup>7</sup>. A new potential in this field, which is traditionally oriented toward two - dimensional nanostructures, is related to the technology of bulk nanocomposites (BNCs) with functional properties similar to those of an intercellular matrix.

It was shown that the electric field of laser radiation may facilitate formation of the framework of carbon nanotubes (CNTs) in the BNC composition <sup>8</sup>. The presence of this framework forms conditions for self-organization (self assembly) of biological tissues, which occurs without human interference, being supported by weak non-covalent (hydrogen, ion) bonds upon hydrophobic interaction of tissues. A similar organization of biological macro molecules in nature occurs, for example, in phospholipids, which are the main components of plasma cellular membranes <sup>9</sup>.

Biological experiments on laboratory animals showed the absence of allergic reactions when laser prepared BNC samples were introduced into rabbit perichondrium. Replacement of a cartilaginous tissue segment with an implanted nanocomposite sample caused its regeneration upon stimulation of active division of cartilaginous cells (chondrocytes), which are generally passive <sup>10</sup>. Thus, using the aforementioned BNCs, one can implement conditions for growing functional biological tissues, similar to those provided by biological matrix. The purpose of this study was to justify the advantages of the medium of laser preparation (laser nanoformation) of bulk composites based on albumin aqueous dispersion (AAD) with CNTs (AAD - CNT) over alternative methods of fabrication for these nanocomposites <sup>11</sup>. In the experiments, the properties of the laser-fabricated BNCs were compared with the characteristics of the composites formed using thermal methods and LED irradiation <sup>11</sup>.

**Experimental Technique:** We performed experiments with an AAD based on bovine serum albumin (BSA) (Amresco, United States) and distilled water. Liquids were dispersed by stirring using a magnetic agitator at a temperature of 20 - 23 °C until albumin was completely dissolved (for 1 - 2 h). The transparent composition obtained after filtering was investigated by absorption spectroscopy in the BSA absorption range ( $\lambda = 200 - 300$  nm). AADs were generally kept in a refrigerator at 5 - 10 °C (to exclude the effect of bacterial flora) for 3 or 4 weeks and under room conditions for 1 or more operating days (depending on the temperature in the room).

Further experiments were performed using an AAD with 25 wt. % BSA, into which multiwall carbon nanotubes (MWCNT's) or single-wall carbon nanotubes (SWCNT's) were incorporated. Multiwall tubes of the Taunit type with a concentration CMWCNT = 0.1 - 0.3 wt. % were grown on metal catalysts by catalytic pyrolysis (CVD process) from a vapour phase: propane-butane mixture heated to 600 - 680 °C <sup>12</sup>. SWCNT I nanotubes were prepared by the HiPCO method from ethanol vapor at a temperature of ~800 °C, with a catalyst (cobalt nanoparticles) located on bulk silicon and quartz substrates.

SWCNT II nanotubes were fabricated in a similar way, with disproportionation on iron clusters obtained with the aid of catalyst  $\text{Fe}(\text{CO})_5$  in a carbon oxide flow transmitted through a heated reactor under high pressure. The catalyst impurity was then removed from nanotubes using fluorination<sup>12</sup>.

When preparing CNT containing AADs (AAD-CNT compositions), the most appropriate technique was found to be ultrasonic dispersion. Exposure to sound at a frequency of 35 kHz in a 2.8-L tank with heater power  $N \sim 0.3$  kW at a temperature below  $30^\circ\text{C}$  lasted  $\sim 1$  h. After compositions were filtered, their quality was estimated from the transparency of the liquid and the shape of the absorption spectrum of the dispersion obtained.

The thermal stability of the AAD-CNT composition (CMWCNT = 0.3 wt. %) positioned in glass test tube with diameter of 10 mm (equipped with a hydraulic lock)  $\sim 15$  cm<sup>3</sup> in volume was investigated by keeping in a thermostat at  $\sim 40^\circ\text{C}$  for  $\sim 85$  h. Closed test tubes with the same AAD-CNT mixture were kept at room temperature for  $\sim 940$  h. The changes observed in the absorption spectra of the liquid in the range from 350 to 1000 nm are related to the partial sedimentation of the solid phase of the dispersion during tests, which does not hinder much the formation of a stable composite **Fig. 1a**.

To determine the photostability of AAD-MWCMT with CMWCNT = 0.1 wt %, we illuminated the compositions by AFS LEDs (Solaris photo-therapeutic apparatus), emitting in three different (UV, red, and near IR) spectral ranges. To this end,  $\sim 20$  mL of liquid were placed in closed cylindrical glass vessels (measuring glasses) with a cross section of  $\sim 4$  cm<sup>2</sup> and illuminated from above; the light sources were located at a distance of  $\sim 50$  mm from the liquid surface and light spot area SIs was  $\sim 55$  cm<sup>2</sup>. Peaks in the emission spectrum were observed at 365 (UV LED, power  $N = 30$  mW), 630 (red LED,  $N = 65$  mW), and 810 (IR LED,  $N = 80$  mW) nm.

The absorption spectra of irradiated AAD-MWCMT were recorded on an SF-26 spectrophotometer for 50 - 60 h, with a time interval of  $\sim 10$  h. The data obtained with a red LED are

presented in **Fig. 1b**. One can see that irradiation of the liquid to a surface dose of  $\sim 0.3$  kJ/cm<sup>2</sup> leads to a monotonic increase in its optical density. A similar change in the optical density of AAD-MWCMT was observed under irradiation with UV and IR LEDs.

In the first series of experiments on preparation of nanocomposites, AAD - MWCMT weights with CMWCNT = 0.1 wt % and a mass of  $\sim 1$  g were placed in closed test tube diameter of 10 mm (liquid column height  $\sim 4$  cm) and kept in a thermostat at a temperature of  $\sim 50^\circ\text{C}$  for 50 - 60 h. At the end of this procedure, solidified composite samples were formed on the bottom of test tubes for a time of 1 - 2 h.

After removing BNC samples from the test tubes and cooling in air, they decomposed into individual small fragments for a short time (from several tens of minutes to several hours). This process was similar to "flaky decay" of dried AAD, accompanied by a conformational change in the protein molecule (wedge shaped dehydration)<sup>13</sup>.

In the second series of experiments, similar AAD-MWCMT samples with a mass of  $\sim 20$  g were placed in an open measuring glass with  $S \sim 4$  cm<sup>2</sup> and illuminated from above by three LEDs (see above) located at a distance of  $\sim 50$  mm from the liquid surface ( $S_{\text{Is}} \approx 55$  cm<sup>2</sup>). After irradiating dispersions for 50 - 60 h and solidifying composite samples, the latter were extracted from the vessels and placed in air. The final result of the second series of experiments fragmentation of composites a short time after cooling was similar to their decomposition observed in the first series of experiments. The nanocomposites obtained from AAD-MWCMT under similar conditions as a result of illumination by a DRUF 125-3 Hg lamp for  $\sim 50$  h behaved similarly.

In the third series of experiments, an AAD-CNT mixture was illuminated using a system based on IR-laser sources: cw diode lasers ( $\lambda_{\text{gen}} = 810$  and  $970$  nm) with a fiber output and power up to 20 W. A measuring glass ( $S \sim 4$  cm<sup>2</sup>) with illuminated liquid was placed in a support on a special table. The laser beam was directed to the liquid surface using the beam of an additional low-power green solid-state laser (second harmonic,  $\lambda_{\text{gen}} = 530$  nm)

transmitted through the same fiber as the main laser beam. Pointing was performed so as to make the laser-spot diameter approximately coincide with the inner diameter of the liquid containing vessel. The dispersion temperature was measured by a thermocouple or a pyrometer.

Laser radiation directed from above along the measuring glass axis was used to evaporate the aqueous component of the dispersion and form a black BNC sample on the bottom of the measuring glass. The quality of the BNC obtained (homogeneous coloring and absence of whitish regions of denatured albumin, as well as their hardness) depended on the illumination intensity and duration; the consistency of the material could be varied from rubberlike (at a lower illumination dose) to glassy. The product mass was generally 50 - 70% smaller than the initial liquid mass.

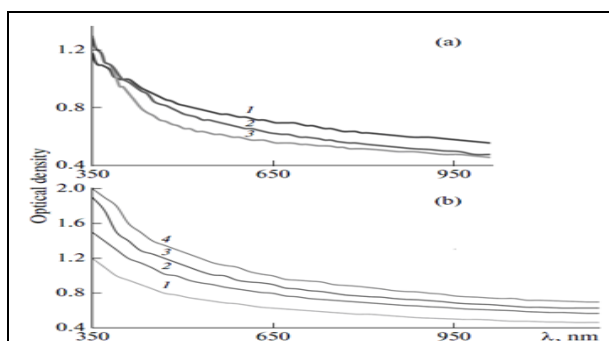


**FIG. 1: ABSORPTION SPECTRA (WITH RESPECT TO WATER) OF 25 wt % AQUEOUS DISPERSION OF BOVINE SERUM ALBUMIN WITH TAUNIT MULTI-WALL CARBON NANOTUBES (CONCENTRATION 0.1 wt %) OBTAINED AFTER (a) long-term storage and thermostating and (b) irradiation of liquids by a red LED. (a) Samples (1) in the initial state, (2) after storage for 938 h, and (3) after thermostating at  $\sim 40$  °C for 83 h and (b) (1-4) after irradiation to doses of (1) 60, (2) 135, (3) 195, and (4) 315 J /cm<sup>2</sup>. The liquid-layer thickness is 1 cm.**

The stability of the BNC obtained under laser irradiation in this series of experiments significantly differed from the unstable behavior (decomposition) of the nanocomposites formed as a result of thermal drying and illumination of the dispersion by LEDs under the above described experimental conditions. This is confirmed by the fact that these BNCs retained their appearance and other properties for several years after preparation. To study the density of the composite samples obtained, we cleaved them into small fragments with linear sizes of 3 - 4 mm (from 10 to 15 pieces for each sample). The sample mass was measured

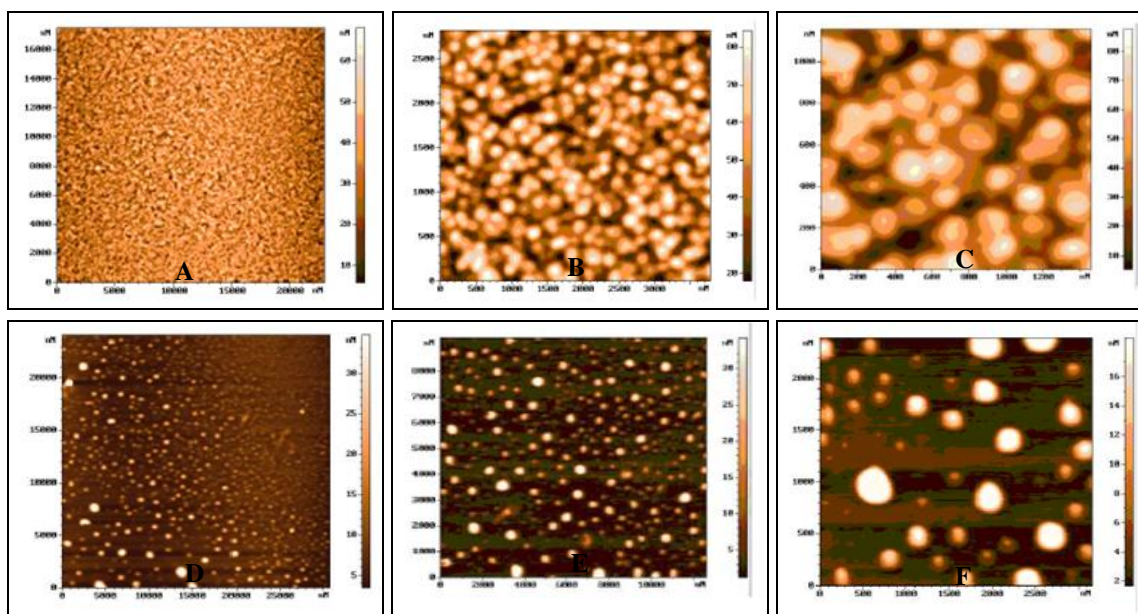
using an analytical balance. These fragments were then immersed in a measuring cylinder, filled with high-purity gasoline by half. The sample volume was calculated using a dimensional scale<sup>14</sup>.

The experimental  $\rho$ -values for MWCMT and SWCNT - based BNCs (the confidence interval for which corresponds to confidence probability  $\alpha = 0.9$ ) are listed in the table in comparison with the data for crystallized BSA hydrate, some widespread structural materials (iron, aluminium, and polymethylmethacrylate (PMMA), and human cortical bone. As can be seen in the table, the  $\rho$  values are similar for all nanocomposites under study. They slightly exceed the albumin hydrate density, are close to the PMMA density, smaller than the aluminium and bone density by a factor of 2 and smaller than the iron density by a factor of about 8. The composite density is approximately the same as water<sup>15</sup>. Composite Vickers hardness Hv was determined on the above described fragments, which were previously ground and polished. Hardness measurements were performed on a PMT-3 micro-hardness meter. The Hv values were calculated by dividing the load applied by the indenter impression surface area.

The experimental Hv values for the composites and structural materials chosen for comparison are listed in the table. The confidence intervals correspond to  $\alpha = 0.9$ . Despite the fact that all BNCs studied had approximately the same density, the hardness of the BNCs prepared by laser irradiation ( $\sim 300$  MPa) significantly exceeded the hardness of the unstable composites ( $\sim 200$  MPa) obtained by other techniques. It was higher than that of albumin hydrate by a factor of about 4; comparable with that of PMMA, iron, and aluminium; and close to the bone hardness **Table 1.** **Fig. 2** shows atomic force microscopy (AFM) topographs of the nanocomposite samples obtained from (a-c) 25% AAD with SWCNT I and (d-f) SWCNT II by laser irradiation, according to the technique. When analyzing these images (their scale increases from left to right), one must take into account possible distortions in the plane coordinates, whereas a more reliable size characteristic of objects is their height, which is depicted by color<sup>15</sup>. As can be seen in **Fig. 2**, cluster partial ordering is a characteristic feature of the structural images of BNCs.

**TABLE 1: DENSITY AND HARDNESS OF MATERIALS**

Materials	Preparation conditions	Density, kg/m <sup>3</sup>	Hardness, MPa
	First series: thermostating	~ 1250	200 ± 20
	Second series: irradiation by LEDs (wavelength, nm)	~ 1300	180 ± 10 (365 nm) 190 ± 20 (630 nm) 220 ± 10 (810 nm) ~ 200 (Hg lamp)
Nanocomposites based on single-layer carbon nanotubes	Third series: laser irradiation (λgen = 0.97 μm)	1250 ± 60	320 ± 60
Nanocomposites based on single-layer carbon nanotubes		1220 ± 80	270 ± 60
Albumin hydrate	Solidification after drying	~1000	~ 70
Annealed iron		~ 9700	~ 250
Aluminium		~ 2800	~ 200
PMMA		~ 1200	~ 200
Native cortical bone		~ 2000	~ 500

**FIG. 2: AFM TOPOGRAPHS OF NANOCOMPOSITE SAMPLES OBTAINED FROM AAD WITH SWCNT I (A-C) AND SWCNT II (D-F) UNDER LASER IRRADIATION. ALL SIZES ARE IN NANOMETERS**

**RESULTS AND DISCUSSION:** Our experimental data indicate the advantages of laser-based preparation (laser nanoformation) of bulk nanocomposites. The mechanical strength of these nanocomposites exceeds the strength of the composites obtained by removing the liquid component of the dispersion upon long term heating and after illuminating the liquid by LEDs emitting in different spectral ranges or by a mercury lamp. According to our observations, the nanocomposites fabricated by laser nanoformation from AAD with carbon nanotubes remain stable for 5 years.

The denaturation temperature for pure BSA is 60 - 70 °C, whereas the laser-fabricated bulk nanocomposites remain stable at much higher temperatures (≤ 200 °C).

The hardness of the BNCs under study (~300 MPa) is combined with their rather low density (1200 - 1300 kg/m<sup>3</sup>, a value close to the water density), which is due to their high porosity. According to the data of <sup>16</sup>, the relative volume of nanopores in such BNCs is 30-55% with their diameters ranging from 25 to 65 nm. The presence of nanopores in the nanocomposites makes them more attractive for medical applications, providing favorable conditions for fusion, migration, and proliferation of cells and channels for blood vessels, as in porous bone tissue <sup>17</sup>. The high strength and durability of BNCs obtained by laser irradiation may be due to the formation of a nanotube framework in their bulk by an electric field of directed laser radiation; this mechanism correlates well with the structural data on these nanocomposites.

According to <sup>17</sup>, CNTs can be oriented (perpendicular to the substrate surface) by the electric field of CO<sub>2</sub> - laser radiation with a power of 30 W at a field strength  $E_l = 10 - 20$  kV/m. At a power density of the diode lasers used in this study ( $10 - 20$  W/cm<sup>2</sup>),  $E_l = 5 - 10$  kV/m. Under these conditions, CNTs are likely to be oriented and, correspondingly, provide conditions for nano-framework formation in BNCs.

In addition, the effect of the laser-radiation electric field on the CNT orientation can be enhanced by the end of nanotubes, depending on the CNT sizes and the character of structurization of the CNT ensemble. Near the CNT end, the light field strength exceeds  $E_l$  by a factor of  $ma + b$ , where aspect ratio  $a = l/d$  ( $l$  and  $d$  are, respectively, the CNT length and diameter) and  $b \approx 30$ . Factor  $m$  is approximately 0.7 for isolated nanotubes and decreases with a decrease in the distance between CNTs <sup>30</sup>. For the SWCNTs and MWCMTs used in our study, the  $a$  values are, respectively,  $\sim 1000$  and  $\leq 50$  <sup>18, 19</sup>.

**CONCLUSION:** The possibility of forming stable materials having high mechanical properties, as compared with other ways for preparing such composites, is a specific feature of the laser nanoformation of BNCs from AAD with CNTs. Their structure is characterized by cluster partial ordering. Orientation of CNTs under the electric field of directed laser radiation forms conditions for building a nanotube framework in nanocomposites; this process may lead to a more efficient self organization of cellular material than in the case of planar CNT structures, on which growth, development, and branching of living nervous, bone, and stem cells is observed.

The biocompatibility of bulk nanocomposites is determined in many respects by the properties of the highly soluble globular protein albumin, which performs a transport function in many living organisms and plants. CNT and albumin complexing (functionalization), which occurs in this case, significantly reduces the nanotube toxicity and may considerably extend the range of safe biomedical application of these BNC's. The results of our study of the stability, density, hardness, and internal structure of the laser-fabricated BNC's indicate that they can be used as

filling materials for surgical implants of wide application.

**ACKNOWLEDGEMENT:** We are very much thankful to Bharat scans Chennai and Saveetha Dental Hospital for providing valuable suggestions to complete this work.

**CONFLICT OF INTEREST:** Nil

## REFERENCES:

1. Galliot B, Crescenzi M, Jacinto A and Tajbaksh S: Trends in tissue repair and regeneration. Development 2017; 144: 357-364. doi: 10.1242/dev.144279.
2. Shafiq M, Jung Y and Kim SH: Insight on stem cell preconditioning and instructive biomaterials to enhance cell adhesion, retention, and engraftment for tissue repair. Biomaterials 2016; 90: 85-115. doi: 10.1016/j.biomaterials.2016.03.020.
3. Tedesco G *et al.*: Composite PEEK / Carbon fiber implants can increase the effectiveness of radiotherapy in the management of spine tumors. J Spine Surg 2017; 3(3): 323-329. doi: 10.21037/jss.2017.06.20.
4. Smeets R *et al.*: Impact of Dental Implant Surface Modifications on Osseointegration. Biomed Res Int. June 2016 1(10) 1155-1171. doi: 10.1155/2016/6285620
5. Muller K *et al.*: Review on the processing and properties of polymer nanocomposites and nanocoatings and their applications in the packaging, automotive and solar energy fields" Nanomaterials (Basel). 2017; 7(4): 74. doi: 10.3390/nano7040074
6. Pannuwat P *et al.*: Biological matrix effects in quantitative tandem mass spectrometry-based analytical methods: advancing biomonitoring. Crit Rev Anal Chem 2016; 46(2): 93-105. doi: 10.1080/10408347.2014.980775
7. Rajendran V *et al.*: Development of nanocomposite materials for biomedical applications. 2nd World Congress on Bio Summit and Molecular Biology Expo Dubai, UAE Scientific Tracks Abstracts: J Biotechnol Biomater 2016; 1(10): 42-49. doi: 10.4172/2155-952X.C1.061
8. Zebrotskova IV: Carbon nanotubes: Sensor properties. A Review February 2016; 2(4): 95-105. doi: 10.1016/j.moem.2017.02.002
9. Himbert S *et al.*: The Molecular Structure of Human Red Blood Cell Membranes from Highly Oriented, Solid Supported Multi-Lamellar Membranes. Scientific Reports 2017; 39661, 2017 Report 7 doi: 10.1038/srep39661
10. Ageeva SA *et al.*: Possible Medical Application of Laser Nanoengineering. Biomedical Engineering 2011; 44(6): 233-236. doi: 10.1007/s10527-011-9195-z
11. Venter M *et al.*: Nanotechnologies in Preventive and Regenerative Medicine. An Emerging Big Picture A volume in Micro and Nano Technologies 2018 First Edition; 93-206. ISBN-10: 0323480632
12. Tripathi PK *et al.*: Synthesis of multi-walled carbon nanotubes from plastic waste using a stainless-steel CVD Reactor as Catalyst. Nanomaterials(Basel). 2017; 7(10): 284. doi: 10.3390/nano7100284
13. Gerasimenko AY *et al.*: A study of preparation techniques and properties of bulk nanocomposites based on aqueous albumin dispersion. Optics and Spectroscopy 2013; 115(2): 283-289 doi: 10.1134/S0030400X13080092

14. Buldem G: Recombinant biosynthesis of bacterial cellulose in genetically modified *Escherichia coli*. *Bioprocess Biosyst Eng* 2018; 41(2): 265-279. doi: 10.1007/s00449-017-1864-1
15. Engenharia CD *et al.*: The use of atomic force microscopy as an important technique to analyze the dispersion of nanometric fillers and morphology in nanocomposites and polymer blends based on elastomers *Polímeros* vol.24 no.6 São Carlos Nov./Dec. 2014; 24(6). <http://dx.doi.org/10.1590/0104-1428.1648>
16. Andreeva IA, Bagratashvili VB, Ichkitidze LI, Podgaetsky VM, Ponomareva OV, Savranskii VV and Selishchev SV: Determination of mechanical properties of biocompatible three - dimensional nanocomposites manufactured using laser methods. *Biomedical Eng* 2010; 43(6): 42-51.
17. Kamanina NV, Vasil'ev PY and Studenov VI: Features nanostructured coatings using laser technology and oriented carbon nanotubes'. *Pis'ma ZhTF* 2011; 37(3): 23-29.
18. Tkachev AG, Mishchenko SV, Negrov VL, Memetov NR, Pas'ko AA, Blinov SV and Turlakov DA: Industrial production of carbon nanomaterial "Tounit". *Nano-industriya* 2007; 2: 24-26.
19. Golikov FV, Pozharov AS, Obratsova ED, Arutyunyan NR, Terekhov SV, Chernov AI, Konov VI, Iskhakova LD and Lobach AS: Synthesis and characterization of single-wall carbon nanotubes grown by chemical deposition of ethanol vapour. *Adv. Sc. Techn* 2006; 48: 31-36.

**How to cite this article:**

Ganesh EN: Carbon nanotube usage in medical applications - review. *Int J Pharm Sci & Res* 2018; 9(7): 2686-92. doi: 10.13040/IJPSR.0975-8232.9(7).2686-92.

All © 2013 are reserved by International Journal of Pharmaceutical Sciences and Research. This Journal licensed under a Creative Commons Attribution-NonCommercial-ShareAlike 3.0 Unported License.

This article can be downloaded to **ANDROID OS** based mobile. Scan QR Code using Code/Bar Scanner from your mobile. (Scanners are available on Google Playstore)